



HAL
open science

Recursive Linear Continuous Quaternion Attitude Estimator From Vector Observations

Jin Wu, Zebo Zhou, Hassen Fourati, Ming Liu

► **To cite this version:**

Jin Wu, Zebo Zhou, Hassen Fourati, Ming Liu. Recursive Linear Continuous Quaternion Attitude Estimator From Vector Observations. *IET Radar Sonar and Navigation*, 2018, 12 (11), pp.1696-1207. 10.1049/iet-rsn.2018.5028 . hal-01923022

HAL Id: hal-01923022

<https://inria.hal.science/hal-01923022>

Submitted on 14 Nov 2018

HAL is a multi-disciplinary open access archive for the deposit and dissemination of scientific research documents, whether they are published or not. The documents may come from teaching and research institutions in France or abroad, or from public or private research centers.

L'archive ouverte pluridisciplinaire **HAL**, est destinée au dépôt et à la diffusion de documents scientifiques de niveau recherche, publiés ou non, émanant des établissements d'enseignement et de recherche français ou étrangers, des laboratoires publics ou privés.

Recursive Linear Continuous Quaternion Attitude Estimator From Vector Observations

Jin Wu^{1,2,3}, Zebo Zhou^{1*}, Hassen Fourati⁴, Ming Liu³

¹ School of Aeronautics and Astronautics, University of Electronic Science and Technology of China, Chengdu, 611731, China

² School of Automation, University of Electronic Science and Technology of China, Chengdu, 611731, China

³ Department of Computer & Electrical Engineering, Hong Kong University of Science and Technology, Hong Kong, China

⁴ Grenoble-Image-Speech-Signal-Automatics Laboratory, Centre National de la Recherche Scientifique, University Grenoble Alpes, Grenoble 38400, France

The source code of this paper has been uploaded to <https://github.com/zarathustr/RLQE>.

* E-mail: klinsmann.zhou@gmail.com

Abstract: Attitude estimation from vector observations is widely employed in aerospace applications for accurate integrated navigation using solutions to Wahba's problem. Wahba's solutions are practical but may corrupt facing critical cases in the presence of almost collinear reference vector measurements, which is inevitable in robotic applications with redundant sensor arrays or platforms with celestial vision sensors in similar directions. Different from existing algorithms, this paper presents a novel sequential multiplicative quaternion attitude estimation method from various vector sensor outputs. The unique linear constitution of the algorithm leads to its specific name of Recursive Linear Quaternion Estimator (RLQE). The algorithm's architecture is designed to use each single pair of vector observation linearly so that the vector observations can be arbitrarily chosen and fused. The closed-form covariance of the RLQE is derived that builds up the existence of a highly reliable RLQE Kalman filter (RLQE-KF). Simulations and experiments are carried out to give the performances of our algorithm and representative ones. Compared with other works, the proposed RLQE maintains good precision, better consistency and lower variance bounds. Moreover, the attitude estimation performance with critical cases is especially much better than conventional Wahba's solution on its continuity, accuracy and variance.

1 Introduction

With the final mission of the Cassini orbiter, this space shuttle faced its burn-up destruction in the atmosphere of Saturn, on Sep 15, 2017 [1, 2]. In the short modern technological history, realizing the long-term voyage of a spacecraft has been extensively investigated. Despite of the existing achievements in flight dynamics and material sciences, navigation has become a kernel tool in complicated space tasks for nowadays advances in integrated circuits and system engineering [3, 4]. Attitude estimation is a key issue inside the navigation because its error significantly determines the accuracy of velocity and position estimates [5, 6]. While for space missions, celestial instrumentation devices including star trackers, X-pulsar sensors are required for accurate results [7]. They are actually always converted to 3-axis vector observations for orientation determination. Attitude estimation is also widely adopted in many areas including human motion tracking, gait analysis, robotics and etc. [8–10]. They integrates the information of various vector observations acquired from one or more sensors. Representative methods can be categorized into the filtering and the batch-processing methods. Filtering methods are constituted by Kalman filtering, complementary filtering, particle filtering, nonlinear observers and etc. [11–15].

Filtering methods for attitude estimation always encounter the problem of nonlinearity as the rotation equalities are always parameterized by Euler angles and quaternions where trigonometric and quadratic functions take place [16]. Commonly, solving this problem leads to the adoption of extended Kalman filter (EKF, [17]), unscented Kalman filter (UKF [18]) and etc. [19]. As nonlinear filtering introduces instability according to the choice of initial covariance and may probably increase the execution time, Wahba's solutions sometimes replace filtering methods for fast computation speed and controllable stability. However, as far as the noise scale is concerned, filtering methods are obviously better than Wahba's solutions in most

cases.

The Wahba's problem has been studied for almost 50 years, which plays an important role in attitude determination [20]. It uses the weights to describe the significances of different vector observations so that the least-square relationship between vector observations is established. Many effective optimal algorithms have been proposed to solve the Wahba's problem e.g. the QUaternion ESTimator (QUEST, [21]), Fast Optimal Attitude Matrix (FOAM, [22]), Singular Value Decomposition (SVD, [23]), the ESTimator Of Quaternion (ESOQ, [24]), our Fast Linear Attitude Estimator (FLAE, [25]) and etc. [26]. To analytically compute eigenvalues and eigenvectors, Yang et al. developed a method using analytic solutions to quartic equation [27]. This method is proved to be efficient and owns almost the same time consumption as that of QUEST. Wahba's problem significantly relies on the weight of each vector observation. And according to theoretical and experimental results in existing literatures [28], when reference vectors are almost collinear, denoting an extreme case with a single vector observation pair, the estimated attitude would be ambiguous and has large determination errors. Such condition, in fact, always occurs due to the installation of sensors like sun sensor, nadir sensor, magnetometer and etc. with a small field-of view [29]. Therefore, for batch processing, existing methods may face dilemma according to these critical cases [30]. Would there be a solution to this problem? It is necessary to develop a new algorithm that can obtain stable, continuous, accurate and robust attitude estimation with one or more vector observation pair(s).

In our previous works [10, 25], we obtain several interesting findings for attitude determination and estimation. These findings are different from conventional solutions. One of them uses the rotation on \mathbb{R}^4 to transform an arbitrary quaternion to the target attitude quaternion by means of accelerometer readings. However, they are not very continuous in practice and too specific for certain sensor combination. Based on these point, we hereinafter present a simple

and comprehensive algorithm that obtains robust and accurate attitude estimation from vector observations. The main contributions are listed as follows:

1. Based on our previous finding, we propose a new quaternion transformation on \mathbb{R}^4 that further gives continuous attitude quaternion estimates from a single vector observation pair.
2. Closed-form covariance propagation of this case is systematically derived. Using the quaternion solution and corresponding variance information, intuitive chain-rule of the multi-vector propagations (RLQE) of attitude quaternion and its covariance are able to be given.
3. System internals are intensively analyzed which shows the disadvantage of the unsupervised fusion equations on the positive definiteness of their covariances. A supervised version is proposed to make the covariances positive definite all the time so that a parallel Kalman filter is able to be further designed to give more smooth estimates.

Simulation and experiments are carried out from many aspects to show the performances of the proposed RLQE. Results indicate that the proposed RLQE is accurate and robust in face of critical cases and sometimes much more time-efficient with respect to representative methods. Real-world robotic validations are also presented to give its superiority in mechatronic navigation, especially the dead-reckoning (DR).

This paper is briefly structured as follows: Section II reviews the previous work we have done for accelerometer and proposes the novel attitude solution from a single vector observation pair. Variance analysis is also given in this section. In section III, the calculation procedure of RLQE is given. The angular rate determination is involved while the initialization of RLQE is discussed as well. Section IV presents the simulations, experiments and results on RLQE, compared with other representative methods. Section V contains the concluding remarks.

2 Background and Our Method

2.1 Brief Background Review

Given a single normalized observation vector $\mathbf{D}^b = (D_x^b, D_y^b, D_z^b)^\top$ in the body frame b and its corresponding normalized reference vector $\mathbf{D}^r = (D_x^r, D_y^r, D_z^r)^\top$ in the reference frame r , we can associate the two vectors with the direction cosine matrix (DCM) \mathbf{C} by

$$\mathbf{D}^b = \mathbf{C}\mathbf{D}^r \quad (1)$$

where the DCM satisfies

$$\mathbf{C} \in SO(3), \mathbf{C}\mathbf{C}^\top = \mathbf{C}^\top\mathbf{C} = \mathbf{I}, \det(\mathbf{C}) = +1 \quad (2)$$

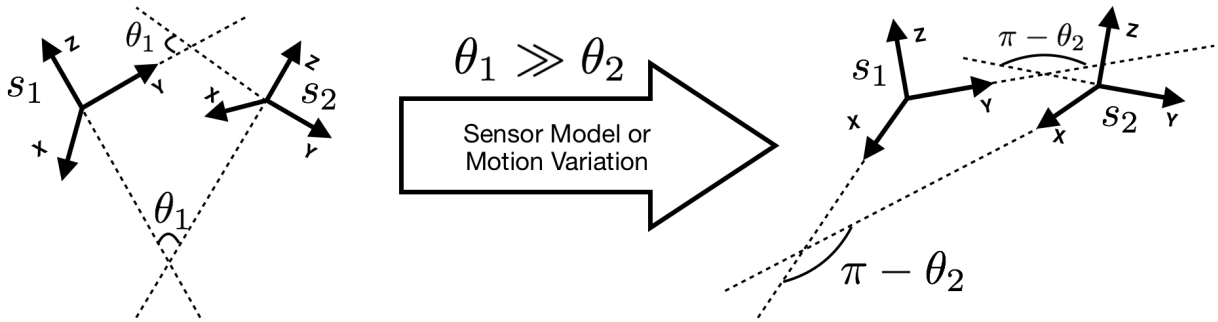


Fig. 1: The gradual evolution of sensor reference frames from large included angle to almost collinear case. s_1 and s_2 are two sensor reference frames while θ_1 and θ_2 are their included angles for two different cases.

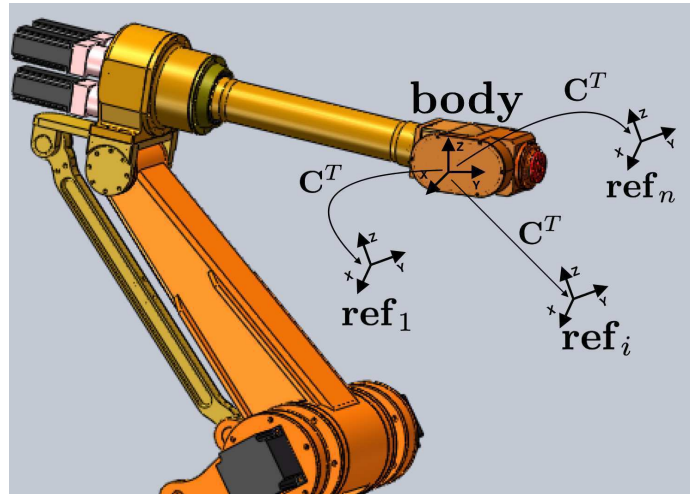


Fig. 2: The diagram that shows the vector observations and their transformations between body frame b on the robotic arm and reference frame r . ref_i denotes the i -th reference vector. \mathbf{C}^\top stands for the inverse rotation from frame r to frame b .

These definitions are also shown in Fig. 2. When there are pairs of vector observations, the corresponding relationship is equivalent to the Wahba's problem, such that it minimizes the following loss function

$$L(\mathbf{C}) = \frac{1}{2} \sum_{i=1}^n a_i \|\mathbf{D}_i^b - \mathbf{C}\mathbf{D}_i^r\|^2, n \geq 2 \quad (3)$$

in which a_i denotes the weight of the i -th vector observation pair. $\|\cdot\|$ is the Euclidean norm. The main break-through of existing Wahba's solutions is to transform the original least-square problem into an eigenvalue-finding problem [31], which is presented as follows

$$\mathcal{K}\mathbf{q} = \lambda_{\max}\mathbf{q} \quad (4)$$

where \mathcal{K} is composed by

$$\mathcal{K} = \begin{bmatrix} \mathbf{S} - \mathbf{I}_{3 \times 3} \text{tr}(\mathbf{B}) & \mathbf{z} \\ \mathbf{z}^\top & \text{tr}(\mathbf{B}) \end{bmatrix} \quad (5)$$

in which

$$\begin{aligned} \mathbf{B} &= \sum_{i=1}^n a_i \mathbf{D}_i^b (\mathbf{D}_i^r)^\top \\ \mathbf{S} &= \mathbf{B} + \mathbf{B}^\top \\ \mathbf{z} &= \sum_{i=1}^n a_i \mathbf{D}_i^b \times \mathbf{D}_i^r \end{aligned} \quad (6)$$

with $tr(\cdot)$ denoting the trace of a certain squared matrix. λ_{max} represents the maximum positive eigenvalue of \mathcal{K} . When there is only one pair of vector observations, it has been discovered that there may have two eigenvectors related to the maximum eigenvalue 1 [28, 32]. In this case, the calculated quaternions are not continuous in the Hamilton space \mathbb{H} , making the calculated quaternion not reliable for fusion or control in later loops. This leads to an authentic critical case when there are two or more same sensors installed on the robotic arm for redundant estimation. An advanced version of critical case is that the reference vectors are set up quite different initially but coincide with each other gradually over time (see Fig. 1). For example, when the two installed star trackers are pointing to the same distant light star, the difference between the two sensors are very small. In the following sub-section, we are going to give the generalized continuous quaternion solution to the single-vector problem, hoping to overcome the shortcoming that Wahba's solutions reserve for the critical cases.

2.2 Continuous Quaternion From A Single Vector Observation Pair

The Wahba's problem can be converted equivalently to obtaining the least-square solution to the system of vector observation pairs and weights [25], such that

$$\begin{cases} \sqrt{a_1}(\mathbf{D}_1^b - \mathbf{C}\mathbf{D}_1^r) = \mathbf{0} \\ \sqrt{a_2}(\mathbf{D}_2^b - \mathbf{C}\mathbf{D}_2^r) = \mathbf{0} \\ \vdots \\ \sqrt{a_n}(\mathbf{D}_n^b - \mathbf{C}\mathbf{D}_n^r) = \mathbf{0} \end{cases} \quad (7)$$

First, we are going to solve the continuity problem. Different from our previous method FLAE [25], motivated by the recursive quaternion kinematic equation, we would like to compute the attitude step-by-step. A continuous rotation on \mathbb{R}^4 from a single vector observation pair is given by [33]:

$$\mathbf{q}_k = \frac{1}{2}(\mathbf{W}_k + \mathbf{I})\mathbf{q}_{k-1} \quad (8)$$

where k stands for the time epoch index. \mathbf{q}_k stands for the fused quaternion at time epoch k ; \mathbf{I} denotes the identity matrix with proper dimension; \mathbf{W}_k is constituted by the vector observation pair sampled at the same time, such that [33]

$$\mathbf{W}_k = D_{x,k}^r \mathbf{M}_1(\mathbf{D}_k^b) + D_{y,k}^r \mathbf{M}_2(\mathbf{D}_k^b) + D_{z,k}^r \mathbf{M}_3(\mathbf{D}_k^b) \quad (9)$$

in which \mathbf{M} is the function of \mathbf{D}^b :

$$\begin{aligned} \mathbf{M}_1(\mathbf{D}_k^b) &= \begin{pmatrix} D_{x,k}^b & 0 & D_{z,k}^b & -D_{y,k}^b \\ 0 & D_{x,k}^b & D_{y,k}^b & D_{z,k}^b \\ D_{z,k}^b & D_{y,k}^b & -D_{x,k}^b & 0 \\ -D_{y,k}^b & D_{z,k}^b & 0 & -D_{x,k}^b \end{pmatrix} \\ \mathbf{M}_2(\mathbf{D}_k^b) &= \begin{pmatrix} D_{y,k}^b & -D_{z,k}^b & 0 & D_{x,k}^b \\ -D_{z,k}^b & -D_{y,k}^b & D_{x,k}^b & 0 \\ 0 & D_{x,k}^b & D_{y,k}^b & D_{z,k}^b \\ D_{x,k}^b & 0 & D_{z,k}^b & -D_{y,k}^b \end{pmatrix} \\ \mathbf{M}_3(\mathbf{D}_k^b) &= \begin{pmatrix} D_{z,k}^b & D_{y,k}^b & -D_{x,k}^b & 0 \\ D_{y,k}^b & -D_{z,k}^b & 0 & D_{x,k}^b \\ -D_{x,k}^b & 0 & -D_{z,k}^b & D_{y,k}^b \\ 0 & D_{x,k}^b & D_{y,k}^b & D_{z,k}^b \end{pmatrix} \end{aligned} \quad (10)$$

provided that $\mathbf{D}_k^b = (D_{x,k}^b, D_{y,k}^b, D_{z,k}^b)^\top$. It is also obtained that [33]

$$\mathbf{K}^\top(\mathbf{q}_{k-1}, \mathbf{D}_k^r) \mathbf{D}_k^b = \mathbf{W}_k \mathbf{q}_{k-1} \quad (11)$$

where

$$\mathbf{K}(\mathbf{q}_{k-1}, \mathbf{D}_k^r) = D_{x,k}^r \mathbf{P}_1(\mathbf{q}_{k-1}) + D_{y,k}^r \mathbf{P}_2(\mathbf{q}_{k-1}) + D_{z,k}^r \mathbf{P}_3(\mathbf{q}_{k-1}) \quad (12)$$

in which

$$\begin{aligned} \mathbf{P}_1(\mathbf{q}_{k-1}) &= \begin{pmatrix} q_0 & q_1 & -q_2 & -q_3 \\ -q_3 & q_2 & q_1 & -q_0 \\ q_2 & q_3 & q_0 & q_1 \end{pmatrix} \\ \mathbf{P}_2(\mathbf{q}_{k-1}) &= \begin{pmatrix} q_3 & q_2 & q_1 & q_0 \\ q_0 & -q_1 & q_2 & -q_3 \\ -q_1 & -q_0 & q_3 & q_2 \end{pmatrix} \\ \mathbf{P}_3(\mathbf{q}_{k-1}) &= \begin{pmatrix} -q_2 & q_3 & -q_0 & q_1 \\ q_1 & q_0 & q_3 & q_2 \\ q_0 & -q_1 & -q_2 & q_3 \end{pmatrix} \end{aligned} \quad (13)$$

with $\mathbf{q}_{k-1} = (q_0, q_1, q_2, q_3)^\top$. In previous main achievements, the multi-vector attitude determination is considered in the classical least-square problem. In fact in robotic applications, the attitude determination is always employed with camera readouts where the reference vectors are regarded as time-varying [34, 35]. In such case, the original problem turn out to be a total least-square (TLS) problem. As discovered by Chang in [36], such problem is equivalent to the classical one. Then we naturally have the following assumptions in this paper:

Assumption 1. *The input signals of excitations from unnormalized vector observations are all finite-power signals, such that*

$$\begin{aligned} 0 &< \lim_{T \rightarrow \infty} \frac{1}{2T} \int_{-T}^T \|\mathbf{D}^b\|^2 dt < +\infty \\ 0 &< \lim_{T \rightarrow \infty} \frac{1}{2T} \int_{-T}^T \|\mathbf{D}^r\|^2 dt < +\infty \end{aligned} \quad (14)$$

and the derivatives of vector observations with respect to time are bounded as well:

$$\begin{aligned} -\infty &< \frac{d\mathbf{D}^b}{dt} < +\infty \\ -\infty &< \frac{d\mathbf{D}^r}{dt} < +\infty \end{aligned} \quad (15)$$

The first assumption is satisfied according to the motion constraint. The second assumption usually holds due to 1) the full measurement ranges of sensors, 2) the possible usage of low-pass and sum filters, 3) the internal sensor kinematics [37].

Assumption 2. *The vector observation pairs are independent with each other i.e.*

$$\Sigma_{\mathbf{D}_i^b, \mathbf{D}_j^b} = \Sigma_{\mathbf{D}_i^r, \mathbf{D}_j^r} = \mathbf{0}, i \neq j \quad (16)$$

where $\Sigma_{\mathcal{A}, \mathcal{B}}$ is the covariance between \mathcal{A} and \mathcal{B} .

Assumption 2 is widely presented in Wahba's solutions e.g. QUEST, FLAE and etc. [21, 25, 36].

(8) is derived from an approximated linear dynamical system. The continuity of this solution is described by the following lemma.

Lemma 1. *For a rigid-body object in continuous motion, with time series of sampled sensor vector observation pairs $\{\mathbf{D}_1^r, \mathbf{D}_2^r, \dots, \mathbf{D}_k^r, \mathbf{D}_{k+1}^r, \dots, \mathbf{D}_n^r\}$, $\{\mathbf{D}_1^b, \mathbf{D}_2^b, \dots, \mathbf{D}_k^b, \mathbf{D}_{k+1}^b, \dots, \mathbf{D}_n^b\}$, where the time period Δt*

between two neighboring pairs are very small, the update equation

$$\mathbf{q}_k = \frac{1}{2} (\mathbf{W}_k + \mathbf{I}) \mathbf{q}_{k-1}, k = 1, 2, \dots, n \quad (17)$$

starting from initial quaternion \mathbf{q}_0 , ensures the computed attitude quaternion to be continuous.

Proof. The differenced quaternion between \mathbf{q}_k and \mathbf{q}_{k-1} can be computed as follows

$$\begin{aligned} \mathbf{q}_k - \mathbf{q}_{k-1} &= \frac{1}{2} (\mathbf{W}_k - \mathbf{I}) \mathbf{q}_{k-1} \\ &= \frac{1}{2} (\mathbf{W}_k - \mathbf{I}) \frac{1}{2} (\mathbf{W}_{k-1} + \mathbf{I}) \mathbf{q}_{k-2} \\ &= \frac{1}{4} (\mathbf{W}_{k-1} + \Delta \mathbf{W} - \mathbf{I}) (\mathbf{W}_{k-1} + \mathbf{I}) \mathbf{q}_{k-2} \\ &= \frac{1}{4} \Delta \mathbf{W}_k (\mathbf{W}_{k-1} + \mathbf{I}) \mathbf{q}_{k-2} \\ &\quad + \frac{1}{4} (\mathbf{W}_{k-1} - \mathbf{I}) (\mathbf{W}_{k-1} + \mathbf{I}) \mathbf{q}_{k-2} \\ &= \frac{1}{4} \Delta \mathbf{W}_k (\mathbf{W}_{k-1} + \mathbf{I}) \mathbf{q}_{k-2} \\ &\quad + \frac{1}{4} (\mathbf{W}_{k-1}^2 - \mathbf{I}) \mathbf{q}_{k-2} \\ &= \frac{1}{4} \Delta \mathbf{W}_k (\mathbf{W}_{k-1} + \mathbf{I}) \mathbf{q}_{k-2} \end{aligned} \quad (18)$$

The derivative of \mathbf{W} satisfies

$$\begin{aligned} \lim_{\Delta t \rightarrow 0} \frac{\Delta \mathbf{W}_k}{\Delta t} &= \frac{d\mathbf{W}_k}{dt} \\ &= \frac{d}{dt} \left[D_{x,k}^r \mathbf{M}_1 (\mathbf{D}_k^b) + D_{y,k}^r \mathbf{M}_2 (\mathbf{D}_k^b) + D_{z,k}^r \mathbf{M}_3 (\mathbf{D}_k^b) \right] \\ &= D_{x,k}^r \frac{d}{dt} \mathbf{M}_1 (\mathbf{D}_k^b) + D_{y,k}^r \frac{d}{dt} \mathbf{M}_2 (\mathbf{D}_k^b) + D_{z,k}^r \frac{d}{dt} \mathbf{M}_3 (\mathbf{D}_k^b) + \\ &\quad \frac{dD_{x,k}^r}{dt} \mathbf{M}_1 (\mathbf{D}_k^b) + \frac{dD_{y,k}^r}{dt} \mathbf{M}_2 (\mathbf{D}_k^b) + \frac{dD_{z,k}^r}{dt} \mathbf{M}_3 (\mathbf{D}_k^b) \end{aligned} \quad (19)$$

Following Assumption 1, the above derivative is bounded. Therefore the derivative

$$\frac{d\mathbf{q}_k}{dt} = \lim_{\Delta t \rightarrow 0} \frac{\mathbf{q}_k - \mathbf{q}_{k-1}}{\Delta t} = \frac{1}{4} \left(\lim_{\Delta t \rightarrow 0} \frac{\Delta \mathbf{W}_k}{\Delta t} \right) (\mathbf{W}_{k-1} + \mathbf{I}) \mathbf{q}_{k-2} \quad (20)$$

always exists and bounded. Then as the quaternion is differentiable, it is definitely continuous as well. ■

2.3 Continuous Quaternion From A Single Vector Observation Pair: Covariance Propagation

Using the \mathbb{R}^4 rotation presented in (8), we are able to obtain the covariance of the quaternion after each update. With the discrete updating equation and letting

$$\mathbf{G}_k = \frac{1}{2} (\mathbf{W}_k + \mathbf{I}) \quad (21)$$

we compute the covariance of \mathbf{q}_k by

$$\begin{aligned} \Sigma_{\mathbf{q}_k} &= E \left\{ \begin{bmatrix} \mathbf{G}_k \mathbf{q}_{k-1} - E(\mathbf{G}_k \mathbf{q}_{k-1}) \\ [\mathbf{G}_k \mathbf{q}_{k-1} - E(\mathbf{G}_k \mathbf{q}_{k-1})]^\top \end{bmatrix} \right\} \\ &= E \left\{ [\mathbf{G}_k \mathbf{q}_{k-1} - \bar{\mathbf{G}}_k \bar{\mathbf{q}}_{k-1}] [\mathbf{G}_k \mathbf{q}_k - \bar{\mathbf{G}}_k \bar{\mathbf{q}}_{k-1}]^\top \right\} \end{aligned} \quad (22)$$

in which

$$\begin{aligned} &\mathbf{G}_k \mathbf{q}_{k-1} - \bar{\mathbf{G}}_k \bar{\mathbf{q}}_{k-1} \\ &= (\bar{\mathbf{G}}_k + \delta \mathbf{G}_k) (\bar{\mathbf{q}}_{k-1} + \delta \mathbf{q}_{k-1}) - \bar{\mathbf{G}}_k \bar{\mathbf{q}}_{k-1} \\ &= \bar{\mathbf{G}}_k \delta \mathbf{q}_{k-1} + \delta \mathbf{G}_k \bar{\mathbf{q}}_{k-1} + \delta \mathbf{G}_k \delta \mathbf{q}_{k-1} \end{aligned} \quad (23)$$

where \bar{x} denotes the mean value of x . Note that the second-order item $\delta \mathbf{G}_k \delta \mathbf{q}_{k-1}$ can be ignored in later computation, the quaternion covariance is calculated by

$$\begin{aligned} \Sigma_{\mathbf{q}_k} &= E \left\{ [\bar{\mathbf{G}}_k \delta \mathbf{q}_{k-1} + \delta \mathbf{G}_k \bar{\mathbf{q}}_{k-1}] [\bar{\mathbf{G}}_k \delta \mathbf{q}_{k-1} + \delta \mathbf{G}_k \bar{\mathbf{q}}_{k-1}]^\top \right\} \\ &= E \left\{ \begin{bmatrix} \bar{\mathbf{G}}_k \delta \mathbf{q}_{k-1} (\delta \mathbf{q}_{k-1})^\top \bar{\mathbf{G}}_k^\top \\ + \delta \mathbf{G}_k \bar{\mathbf{q}}_{k-1} (\delta \mathbf{q}_{k-1})^\top \bar{\mathbf{G}}_k^\top \\ + \bar{\mathbf{G}}_k \delta \mathbf{q}_{k-1} \bar{\mathbf{q}}_{k-1}^\top (\delta \mathbf{G}_k)^\top \\ + \delta \mathbf{G}_k \bar{\mathbf{q}}_{k-1} \bar{\mathbf{q}}_{k-1}^\top (\delta \mathbf{G}_k)^\top \end{bmatrix} \right\} \end{aligned} \quad (24)$$

Two items i.e. $\delta \mathbf{G}_k \bar{\mathbf{q}}_{k-1} (\delta \mathbf{q}_{k-1})^\top \bar{\mathbf{G}}_k^\top$, $\bar{\mathbf{G}}_k \delta \mathbf{q}_{k-1} \bar{\mathbf{q}}_{k-1}^\top (\delta \mathbf{G}_k)^\top$ equal to zeros since there is no correlation between current vector observation and estimated quaternion in last epoch. Finally, the covariance arrives at

$$\begin{aligned} \Sigma_{\mathbf{q}_k} &= \mathbf{G}_k \Sigma_{\mathbf{q}_{k-1}} \mathbf{G}_k^\top + \frac{1}{4} E \left[\delta \mathbf{W}_k \bar{\mathbf{q}}_{k-1} \bar{\mathbf{q}}_{k-1}^\top (\delta \mathbf{W}_k)^\top \right] \\ &= \frac{1}{4} \left[(\mathbf{W}_k + \mathbf{I}) \Sigma_{\mathbf{q}_{k-1}} (\mathbf{W}_k + \mathbf{I}) \right. \\ &\quad \left. + \mathbf{K}^\top (\mathbf{q}_{k-1}, \mathbf{D}_k^r) \Sigma_{\mathbf{D}_k^b} \mathbf{K} (\mathbf{q}_{k-1}, \mathbf{D}_k^r) \right] \end{aligned} \quad (25)$$

where

$$\delta \mathbf{G}_k \bar{\mathbf{q}}_{k-1} = \frac{1}{2} \delta \mathbf{W}_k \bar{\mathbf{q}}_{k-1} = \frac{1}{2} \mathbf{K}^\top (\mathbf{q}_{k-1}, \mathbf{D}_k^r) \delta \mathbf{D}_k^b \quad (26)$$

is invoked.

Lemma 2. The quaternion covariance propagation in (25) is rank-deficient and semidefinite.

Proof. In the first item, we have

$$\begin{aligned} \lambda_{\mathbf{W}_k,1} &= \lambda_{\mathbf{W}_k,2} = 1 \\ \lambda_{\mathbf{W}_k,3} &= \lambda_{\mathbf{W}_k,4} = -1 \end{aligned} \quad (27)$$

since [28, 33]

$$\mathbf{W}_k = \mathbf{W}_k^\top, \mathbf{W}_k^2 = \mathbf{I}, \mathbf{W}_k \mathbf{q}_k = \mathbf{q}_k \quad (28)$$

Therefore, $(\mathbf{W}_k + \mathbf{I}) \Sigma_{\mathbf{q}_{k-1}} (\mathbf{W}_k + \mathbf{I})$ has the rank of 2 and is semidefinite. In another item, $\Sigma_{\mathbf{D}_k^b}$ is defined to be definite. Hence

$$\text{rank}(\Sigma_{\mathbf{D}_k^b}) = 3 \quad (29)$$

Meanwhile, we have

$$\text{rank} \left[\mathbf{K}^\top (\mathbf{q}_{k-1}, \mathbf{D}_k^r) \right] = 3 \quad (30)$$

Then it is obtained that

$$\begin{aligned} &\text{rank} \left[\mathbf{K}^\top (\mathbf{q}_{k-1}, \mathbf{D}_k^r) \mathbf{D}_k^b \right] = \\ &\min \left\{ \text{rank} \left[\mathbf{K}^\top (\mathbf{q}_{k-1}, \mathbf{D}_k^r) \right], \text{rank} \left(\mathbf{D}_k^b \right) \right\} = 3 \end{aligned} \quad (31)$$

Likewise we have

$$\text{rank} \left[\mathbf{K}^\top (\mathbf{q}_{k-1}, \mathbf{D}_k^r) \mathbf{D}_k^b \mathbf{K} (\mathbf{q}_{k-1}, \mathbf{D}_k^r) \right] = 3 \quad (32)$$

While $\mathbf{K}^\top (\mathbf{q}_{k-1}, \mathbf{D}_k^r) \mathbf{D}_k^b \mathbf{K} (\mathbf{q}_{k-1}, \mathbf{D}_k^r)$ is a 4×4 matrix. Hence it is rank deficient. Besides, as this matrix is in quadratic form, its first 3 eigenvalues should be similar with that of $\Sigma_{\mathbf{D}_k^b}$ i.e. they are

positive values. However, as $\mathbf{K}^\top(\mathbf{q}_{k-1}, \mathbf{D}_k^r) \mathbf{D}_k^b \mathbf{K}(\mathbf{q}_{k-1}, \mathbf{D}_k^r)$ is proved to be singular, its 4th eigenvalue should definitely be 0. This proves that $\mathbf{K}^\top(\mathbf{q}_{k-1}, \mathbf{D}_k^r) \mathbf{D}_k^b \mathbf{K}(\mathbf{q}_{k-1}, \mathbf{D}_k^r)$ is semidefinite, as well. Combining the ranks and positive definiteness of the two items, the overall covariance is semidefinite. ■

Remark 1. The above lemma sets a gap to the covariance since it is semidefinite all the time. Such property would be harmful to those systems with observation covariance requirements e.g. the Kalman filter. In classical Kalman filter, when the process and observation covariance matrices are both semidefinite, the filtered states and their covariances are assumed to be critically stable. That is to say, in this occasion, the filtering is unhealthy. In the following lemma, the quaternion propagation is revised to ensure positive definite covariances.

Lemma 3. *The supervised transformation $\mathbf{q}_k = \frac{1}{j} [\mathbf{W}_k + (j-1)\mathbf{I}] \mathbf{q}_{k-1}$ obtains the same stable solution over iterations but may generate covariance matrices with much more positive definiteness, in which the refinement constant j denotes an arbitrary natural number satisfying $j > 2$.*

Proof. The recursive quaternion solution, as described in (8), can be transformed by

$$\begin{aligned} 2\mathbf{q}_k &= (\mathbf{W}_k + \mathbf{I}) \mathbf{q}_{k-1} \\ \Rightarrow j\mathbf{q}_k &= (\mathbf{W}_k + \mathbf{I}) \mathbf{q}_{k-1} + (j-2)\mathbf{q}_k \\ \Rightarrow j\mathbf{q}_k &\approx [\mathbf{W}_k + (j-1)\mathbf{I}] \mathbf{q}_{k-1} \end{aligned} \quad (33)$$

The above approximation is accurate when the sampling period is small. When such condition does not exist, there be tiny differences, with which, however, the global convergence is not affected since at steady state the quaternions at neighbouring time epochs are exactly the same. As shown in Lemma 2, $\mathbf{W}_k + \mathbf{I}$ is semidefinite which leads to the semi-definiteness of quaternion covariance. Here, letting $\mathbf{G}_k = \frac{1}{j} [\mathbf{W}_k + (j-1)\mathbf{I}]$, with $\delta\mathbf{G}_k = \frac{1}{j} \delta\mathbf{W}_k$, the quaternion covariance is derived to

$$\Sigma_{\mathbf{q}_k} = \frac{1}{j^2} \left\{ \begin{array}{l} [\mathbf{W}_k + (j-1)\mathbf{I}] \Sigma_{\mathbf{q}_{k-1}} [\mathbf{W}_k + (j-1)\mathbf{I}] \\ + \mathbf{K}^\top(\mathbf{q}_{k-1}, \mathbf{D}_k^r) \Sigma_{\mathbf{D}_k^b} \mathbf{K}(\mathbf{q}_{k-1}, \mathbf{D}_k^r) \end{array} \right\} \quad (34)$$

We can see that this result ensures the obtained covariance positive definite if the initial quaternion covariance is given to be positive definite. The stable solution to the revised form does not alter since they are identical to the same eigen system $\mathbf{W}_k \mathbf{q}_k = \mathbf{q}_k$. ■

3 Quaternion and Angular Rate from Vector Observation Pairs

3.1 Recursive Linear Quaternion Estimator (RLQE)

The quaternion estimation from vector observation pairs can be treated as the recursive rotation from each single pair. Assume that we currently have n pairs of vector observations. Using the quaternion propagation in (17) and the variance propagation in (33), we obtain the following chain rule

$$\mathcal{R} : \left\{ \begin{array}{l} \mathbf{q}_{k,1}^- = \frac{1}{j_1} [\mathbf{W}_{k,1} + (j_1-1)\mathbf{I}] \mathbf{q}_{k-1}, \mathbf{q}_{k,1} = \mathcal{Y}(\mathbf{q}_{k,1}^-) \\ \mathbf{q}_{k,2}^- = \frac{1}{j_2} [\mathbf{W}_{k,2} + (j_2-1)\mathbf{I}] \mathbf{q}_{k,1}, \mathbf{q}_{k,2} = \mathcal{Y}(\mathbf{q}_{k,2}^-) \\ \vdots \\ \mathbf{q}_{k,n}^- = \frac{1}{j_n} [\mathbf{W}_{k,n} + (j_n-1)\mathbf{I}] \mathbf{q}_{k,n-1}, \mathbf{q}_{k,n} = \mathcal{Y}(\mathbf{q}_{k,n}^-) \\ \mathbf{q}_k = \mathbf{q}_{k,n} \end{array} \right. \quad (35)$$

with $n = 1, 2, \dots$, where $\mathbf{q}_{k,i}$ stands for the quaternion at time epoch k which is undertaking fusion from i -th sensor. \mathbf{q}^- is the forecasted quaternion. j_i is the i -th refinement constant for possible positive-definiteness of covariance. $\mathcal{Y}(\mathbf{q}) = \frac{\mathbf{q}}{\|\mathbf{q}\|}$ is the normalization operator on \mathbb{R}^4 . We define this quaternion propagation function as

$$\mathbf{q}_k = \mathcal{R} \left(\mathbf{q}_{k-1}, \left\{ \mathbf{D}_{k,i}^b, \mathbf{D}_{k,i}^r \mid i = 1, 2, \dots, n \right\} \right) \quad (36)$$

where $\mathbf{D}_{k,i}$ is the vector observation from i -th sensor at time epoch k that leads to $\mathbf{W}_{k,i}$. With each single pair of vector observations, the covariance is propagated independently under the Assumption 2. Then, the covariance propagation's chain rule is given by

$$\mathcal{R}_\Sigma : \left\{ \begin{array}{l} \Sigma_{\mathbf{q}_{k,1}} = \frac{1}{j_1^2} \left\{ \begin{array}{l} [\mathbf{W}_{k,1} + (j_1-1)\mathbf{I}] \Sigma_{\mathbf{q}_{k-1}} \\ [\mathbf{W}_{k,1} + (j_1-1)\mathbf{I}] \\ + \mathbf{K}^\top(\mathbf{q}_{k-1}, \mathbf{D}_{k,1}^r) \Sigma_{\mathbf{D}_{k,1}^b} \\ \mathbf{K}(\mathbf{q}_{k-1}, \mathbf{D}_{k,1}^r) \end{array} \right\} \\ \Sigma_{\mathbf{q}_{k,2}} = \frac{1}{j_2^2} \left\{ \begin{array}{l} [\mathbf{W}_{k,2} + (j_2-1)\mathbf{I}] \Sigma_{\mathbf{q}_{k,1}} \\ [\mathbf{W}_{k,2} + (j_2-1)\mathbf{I}] \\ + \mathbf{K}^\top(\mathbf{q}_{k,1}, \mathbf{D}_{k,2}^r) \Sigma_{\mathbf{D}_{k,2}^b} \\ \mathbf{K}(\mathbf{q}_{k,1}, \mathbf{D}_{k,2}^r) \end{array} \right\} \\ \vdots \\ \Sigma_{\mathbf{q}_{k,n}} = \frac{1}{j_n^2} \left\{ \begin{array}{l} [\mathbf{W}_{k,n} + (j_n-1)\mathbf{I}] \Sigma_{\mathbf{q}_{k,n-1}} \\ [\mathbf{W}_{k,n} + (j_n-1)\mathbf{I}] \\ + \mathbf{K}^\top(\mathbf{q}_{k,n-1}, \mathbf{D}_{k,n}^r) \Sigma_{\mathbf{D}_{k,n}^b} \\ \mathbf{K}(\mathbf{q}_{k,n-1}, \mathbf{D}_{k,n}^r) \end{array} \right\} \\ \Sigma_{\mathbf{q}_k} = \Sigma_{\mathbf{q}_{k,n}} \end{array} \right. \quad (37)$$

which is defined as the function

$$\Sigma_{\mathbf{q}_k} = \mathcal{R}_\Sigma \left(\Sigma_{\mathbf{q}_{k-1}}, \mathbf{q}_{k-1}, \left\{ \mathbf{D}_{k,i}^b, \mathbf{D}_{k,i}^r \mid i = 1, 2, \dots, n \right\} \right) \quad (38)$$

The variance bounds of the quaternions are computed then with

$$\text{diag}(\sigma_{q_{0,k}}, \sigma_{q_{1,k}}, \sigma_{q_{2,k}}, \sigma_{q_{3,k}}) = \pm \sqrt{\text{diag}(\Sigma_{\mathbf{q}_k})} \quad (39)$$

in which $\text{diag}(\Sigma_{\mathbf{q}_k})$ extracts the diagonal elements of $\Sigma_{\mathbf{q}_k}$.

3.2 Angular Rate Estimation from Strapdown Sensors

Using the obtained quaternions, the angular rate determination is also able to be computed in case of emergency incidents e.g. gyroscope failure. The first-order quaternion kinematic equation is given by [14]

$$\frac{d\mathbf{q}_\omega}{dt} = \frac{1}{2} \mathbf{q}_\omega \otimes \varpi \quad (40)$$

where \otimes denotes the quaternion product, $\varpi = (0, \omega^\top)^\top$ with the angular rate of $\omega = (\omega_x, \omega_y, \omega_z)^\top$. Rewriting (40), namely expanding the quaternion multiplication, we have

$$\frac{d\mathbf{q}_\omega}{dt} = \frac{1}{2} \mathbf{q}_\omega \otimes \varpi = \frac{1}{2} \begin{pmatrix} q_0 & -q_1 & -q_2 & -q_3 \\ q_1 & q_0 & -q_3 & q_2 \\ q_2 & q_3 & q_0 & -q_1 \\ q_3 & -q_2 & q_1 & q_0 \end{pmatrix} \varpi \quad (41)$$

Then the angular rate is easily obtained by quaternion inversion:

$$\begin{aligned}\varpi_{v,k} &= 2\mathbf{q}_{v,k}^{-1} \otimes \frac{d\mathbf{q}_{v,k}}{dt} \\ &= 2\mathbf{q}_{v,k}^* \otimes \frac{d\mathbf{q}_{v,k}}{dt} = 2\mathbf{U}\mathbf{q}_{v,k} \otimes \left[\frac{\mathcal{R}(\mathbf{q}_{v,k-1}) - \mathbf{q}_{v,k-1}}{\Delta t} \right] \quad (42)\end{aligned}$$

$$\mathbf{U} = \text{diag}(1, -1, -1, -1)$$

where $\mathbf{q}_{v,k}$ denotes the quaternion from vector observations at time epoch k while $*$ represents the conjugate quaternion. The later 3 components of ϖ_v constitute the angular rate ω .

3.3 Initialization of RLQE

The initial quaternion significantly determines the quality of the starting state of the attitude estimator. A well-initialized attitude quaternion is calculated by

$$\begin{aligned}\mathbf{q}_0^m &= \mathcal{R}\left(\mathbf{q}_0^{m-1}, \left\{ \mathbf{D}_{0,i}^b, \mathbf{D}_{0,i}^r \mid i = 1, 2, \dots, n \right\}\right) \\ \Sigma_{\mathbf{q}_0^m} &= \mathcal{R}_\Sigma\left(\Sigma_{\mathbf{q}_0^{m-1}}, \mathbf{q}_0^{m-1}, \left\{ \mathbf{D}_{0,i}^b, \mathbf{D}_{0,i}^r \mid i = 1, 2, \dots, n \right\}\right) \quad (43)\end{aligned}$$

considering halt when

$$\left\| \mathbf{q}_0^m - \mathbf{q}_0^{m-1} \right\| < \eta \quad (44)$$

where m stands for the step index of the initialization process and η denotes the relative initialization accuracy. Normally, the uninitiated quaternion \mathbf{q}_0^0 can be chosen as $(1, 0, 0, 0)^\top$.

3.4 Outlier Rejection Law

In engineering practice, not all the sensors can meet the certain project's requirements. When using such sensor combinations, an outlier rejection law is needed to reject sensor outliers. These outliers may be induced by mechanical vibration, sudden voltage jumping on ADC e.g. ESD, fatigue failure, model errors and etc. [38, 39]. As the rate gyroscope is usually the most secure device onboard, it is feasible to compare the angular rate estimated from vector observation pairs with the gyro measurements. In static mode, the signal-noise ratio (SNR) is very low according to the absence of noise. However, when the measurement unit is operated in motion, the SNR significantly increases. At this moment, we may empirically deduce the sensor failure by

$$\|\omega_v - \omega\| \begin{cases} Pass < c \\ Fail \geq c \end{cases} \quad (45)$$

where c is an empirical constant defined according to the motion, which is also related to sensor bias. In this way, sensors with outliers can be exempted from being in the fusion process.

3.5 Kalman Filtering (RLQE-KF)

Seen from the chain rules presented in (35) and (37), a common thinking is to design a system and adopts Kalman filtering to achieve optimal state estimation [40]. To avoid cross-correlation between the process and observation model, the RLQE quaternion and that in process model are separated. Defining the state vector as the quaternion, the system dynamics can be represented by [41]

$$\begin{aligned}\frac{d\mathbf{q}}{dt} &= \frac{1}{2} [\boldsymbol{\Omega} \times] \mathbf{q} \\ \Rightarrow \mathbf{q}_k &= \Phi_{k,k-1} \mathbf{q}_{k-1} + \Gamma_k \xi_k \quad (46)\end{aligned}$$

where the transition matrix $\Phi_{k,k-1}$, noise ξ_k and noise matrix Γ_k are given by

$$\begin{aligned}\Phi_{k,k-1} &= \frac{\Delta t}{2} [\boldsymbol{\Omega} \times] + \mathbf{I} \\ \xi_k &= \delta\omega, \Gamma_k = -\frac{\Delta t}{2} \Xi \quad (47)\end{aligned}$$

with last estimated quaternion

$$\Xi_t = \begin{pmatrix} q_1 & q_2 & q_3 \\ -q_0 & -q_3 & -q_2 \\ q_2 & -q_0 & -q_1 \\ -q_2 & q_1 & -q_0 \end{pmatrix} \quad (48)$$

The measurement quaternion in observation vector is parallel with the process quaternion. The discrete observation model is given by

$$\mathbf{q}_{meas,k} = \mathbf{H}_k \mathbf{q}_k + v_k \quad (49)$$

where $\mathbf{q}_{meas,k} = \mathcal{R}(\mathbf{q}_{meas,k-1})$, $\mathbf{H}_k = \mathbf{I}$ and v_k is the noise item. Then the stochastic model can be given by

$$\begin{aligned}\Sigma_{\xi_k} &= \Sigma_{gyro} = \text{diag}(\sigma_{gyro,x}^2, \sigma_{gyro,y}^2, \sigma_{gyro,z}^2) \\ \Sigma_{v_k} &= \mathcal{R}_\Sigma(\Sigma_{\mathbf{q}_{meas,k-1}}) \quad (50)\end{aligned}$$

where $\sigma_{gyro,i}$ is standard deviation of gyro readouts of i -th axis. Since the process and observations models are independent, the classical Kalman update equations can be applied, such that

$$\begin{aligned}\mathbf{q}_k^- &= \Phi_{k,k-1} \hat{\mathbf{q}}_{k-1} \\ \Sigma_{\mathbf{q}_k^-} &= \Phi_{k,k-1} \Sigma_{\hat{\mathbf{q}}_{k-1}} \Phi_{k,k-1}^\top + \Gamma_k \Sigma_{\xi_k} \Gamma_k^\top \\ \mathbf{K}_k &= \Sigma_{\mathbf{q}_k^-} \mathbf{H}_k^\top \left(\mathbf{H}_k \Sigma_{\mathbf{q}_k^-} \mathbf{H}_k^\top + \Sigma_{v_k} \right)^{-1} \\ \hat{\mathbf{q}}_k &= \mathbf{q}_k^- + \mathbf{K}_k (\mathbf{q}_{meas,k} - \mathbf{q}_k^-) \\ \Sigma_{\hat{\mathbf{q}}_k} &= (\mathbf{I} - \mathbf{K}_k \mathbf{H}_k) \Sigma_{\mathbf{q}_k^-} (\mathbf{I} - \mathbf{K}_k \mathbf{H}_k)^\top + \mathbf{K}_k \Sigma_{v_k} \mathbf{K}_k^\top \quad (51)\end{aligned}$$

where \mathbf{K}_k is the Kalman filter and $\hat{\mathbf{q}}$ stands for estimated quaternion. The last equation that computes the covariance of estimated quaternion is actually in the 'Joseph form' ensuring the symmetry and positive definiteness [42].

Remark 2. In this section, there are many parameters regarding the implementation of the algorithms. First, for the RLQE, the refinement constants are very important for the positive definiteness of the covariance. When in real programming, the user can commonly set the values to 3 since under such constraint the covariance is always positive definite. The relative initialization accuracy η is in fact determined by the user's demands and the maximum initial alignment precision [43]. In principle, this constant can be given with some testing experiments. In the outlier rejection law, the threshold c is decided by the relative motion difference. One can obtain this value by rotating the inertial measurement device on specific platforms and compare the ideal angular rates and that from the vector observations. That is to say, this parameter is deduced by the response performance [44]. In general, for RLQE and RLQE-KF, the sensor variances should be pre-determined by large amount of statistics of raw readouts. It should be noted that the initial sensor variance values are very vital to the system. Improper settings may let the RLQE produce much larger variance bounds, which significantly decreases the further filtering accuracy for Kalman filter. With the above proper settings of the parameters, it is able to obtain highly precise attitude estimation results in engineering. The overall implementation is summarized in Algorithm 1.

Algorithm 1 The Recursive Linear Quaternion Estimator (RLQE) and its parallel Kalman filter.

1. Preliminary:

Numbers of available sensors: n
 Relative initialization accuracy: η
 Static mode indicator (angular rates): χ
 Flag that enables the Kalman filter: **EN_KF**
 Vector Observation updated flag: **EN_VEC**
 RLQE updated flag: **EN_RLQE**

2. Initialization:

1. RLQE Initialization:

- (a) $k = 0, m = 1, \mathbf{q}_0^0 = (1, 0, 0, 0)^\top, \Sigma_{\mathbf{q}_0^0} = \mathbf{0}$.
 - (b) Get normalized sensor samples: $\{\mathbf{D}_{0,i}^b, \mathbf{D}_{0,i}^r | i = 1, 2, \dots, n\}$.
 - (c) **while** $\|\mathbf{q}_k^m - \mathbf{q}_k^{m-1}\| > \eta$ **do**
 $\mathbf{q}_0^m = \mathcal{R}\left(\mathbf{q}_0^{m-1}, \{\mathbf{D}_{0,i}^b, \mathbf{D}_{0,i}^r | i = 1, 2, \dots, n\}\right), \Sigma_{\mathbf{q}_0^m} = \mathcal{R}_\Sigma\left(\Sigma_{\mathbf{q}_0^{m-1}}, \mathbf{q}_0^{m-1}, \{\mathbf{D}_{0,i}^b, \mathbf{D}_{0,i}^r | i = 1, 2, \dots, n\}\right), m = m + 1$.
 - (d) $\mathbf{q}_{\text{RLQE},0} = \mathbf{q}_0^m, \Sigma_{\mathbf{q}_{\text{RLQE},0}} = \Sigma_{\mathbf{q}_0^m}$.
2. Kalman Filter Initialization (**EN_KF = TRUE**): $\hat{\mathbf{q}}_{\text{KF},0} = \mathbf{q}_{\text{RLQE},0}, \Sigma_{\hat{\mathbf{q}}_{\text{KF},0}} = \Sigma_{\mathbf{q}_{\text{RLQE},0}}$.

3. Main Loop:

while no halt command received **do**

- 1. $k = k + 1$
- 2. **If EN_KF = TRUE**, Inertial Forecast:
 (a) Get angular rates: $\omega_k = (\omega_{x,k}, \omega_{y,k}, \omega_{z,k})^\top$.
 $\mathbf{q}_{\text{KF},k}^- = \Phi_{k,k-1} \hat{\mathbf{q}}_{\text{KF},k-1}$
- (b) $\Sigma_{\mathbf{q}_{\text{KF},k}^-} = \Phi_{k,k-1} \Sigma_{\hat{\mathbf{q}}_{\text{KF},k-1}} \Phi_{k,k-1}^\top$
- 3. **If EN_VEC = TRUE**, RLQE Propagation:
 (a) Get p_k pairs of normalized sensor samples:
 $\{\mathbf{D}_{k,i}^b, \mathbf{D}_{k,i}^r | i = 1, 2, \dots, p_k\}$.
- (b) Set empirical outlier rejection thresholds: $\{c_i | i = 1, 2, \dots, p_k\}$.
- (c) $\mathbf{q}_{\text{RLQE},k,0} = \mathbf{q}_{\text{RLQE},k-1}$, Valid fusion counter $\mu = 0$.

- d) **For** $i = 1$ **To** p_k
 $\mathbf{q}_{\text{RLQE},k,i} = \mathcal{R}\left(\mathbf{q}_{\text{RLQE},k,i-1}, \{\mathbf{D}_{k,i}^b, \mathbf{D}_{k,i}^r\}\right)$
 $\Sigma_{\mathbf{q}_{\text{RLQE},k,i}} = \mathcal{R}_\Sigma\left(\Sigma_{\mathbf{q}_{\text{RLQE},k,i-1}}, \mathbf{q}_{\text{RLQE},k,i-1}, \{\mathbf{D}_{k,i}^b, \mathbf{D}_{k,i}^r\}\right)$
 $\varpi_{\text{RLQE},k,i} = 2\mathbf{U}\mathbf{q}_{\text{RLQE},k,i} \otimes \left[\frac{\mathbf{q}_{\text{RLQE},k,i} - \mathbf{q}_{\text{RLQE},k,i-1}}{\Delta t}\right]$
If $\|\omega_k\| > \chi$ **and** $\|\varpi_{\text{RLQE},k,i} - \omega_k\| \geq c_i$:
 $\mathbf{q}_{\text{RLQE},k,i} = \mathbf{q}_{\text{RLQE},k,i-1}$
 $\Sigma_{\mathbf{q}_{\text{RLQE},k,i}} = \Sigma_{\mathbf{q}_{\text{RLQE},k,i-1}}$
Else: $\mu = \mu + 1$.
 - e)
 i **If** $\mu > 0$: **EN_RLQE = TRUE**.
 ii **Else**: **EN_RLQE = FALSE**.
 $\mathbf{q}_{\text{RLQE},k} = \mathbf{q}_{\text{RLQE},k,p_k}$
 $\Sigma_{\mathbf{q}_{\text{RLQE},k}} = \Sigma_{\mathbf{q}_{\text{RLQE},k,p_k}}$
 - 4) **If EN_KF = TRUE and EN_RLQE = TRUE**, Kalman Correction:
 $\mathbf{K}_k = \Sigma_{\mathbf{q}_{\text{KF},k}^-} \left(\Sigma_{\mathbf{q}_{\text{KF},k}^-} + \Sigma_{\mathbf{q}_{\text{RLQE},k}}\right)^{-1}$
 $\hat{\mathbf{q}}_{\text{KF},k} = \mathbf{q}_{\text{KF},k}^- + \mathbf{K}_k \left(\mathbf{q}_{\text{RLQE},k} - \mathbf{q}_{\text{KF},k}^-\right)$
 $\Sigma_{\hat{\mathbf{q}}_{\text{KF},k}} = (\mathbf{I} - \mathbf{K}_k) \Sigma_{\mathbf{q}_{\text{KF},k}^-} (\mathbf{I} - \mathbf{K}_k)^\top + \mathbf{K}_k \Sigma_{\mathbf{q}_{\text{RLQE},k}} \mathbf{K}_k^\top$
 $\hat{\mathbf{q}}_{\text{KF},k} = \mathcal{V}(\hat{\mathbf{q}}_{\text{KF},k})$
 - 5) **Output:**
 (a) **If EN_KF = TRUE and EN_RLQE = TRUE**:
 $\mathbf{q}_k = \hat{\mathbf{q}}_{\text{KF},k}$.
 (b) **Else If EN_KF = TRUE and EN_RLQE = TRUE**:
 $\mathbf{q}_k = \mathcal{V}(\hat{\mathbf{q}}_{\text{KF},k}^-)$.
 (c) **Else If EN_KF = FALSE and EN_RLQE = TRUE**:
 $\mathbf{q}_k = \mathbf{q}_{\text{RLQE},k}$.
- end while**

for visual demonstrations. Time consumption of different algorithms is collected using the MATLAB's internal timer.

4 Simulations, Experiments and Results

4.1 Experiments

In this section, the experimental validation and comparisons are finished using our designed hardware platform. This platform is constituted of a dual-core micro controller, several wireless transmitters, one high precision 3DM-GX3-25 inertial measurement unit (IMU) produced by MicroStrain, LORD Inc. and a high-end attitude and heading reference system (AHRS) produced by Siyue Inc., Shanghai, China. Using the calibration software of the two main units, the sensor biases of internal gyroscopes, accelerometers and magnetometers are calculated and cancelled. The micro controller is based on STMicroelectronics STM32F4-series chips with several programmable interfaces like SPI, I2C, UART, CAN and etc., allowing for high-frequency data sampling, processing and transmission. The wireless transmitters make the system more interactive with the upper monitor on PC. Raw inertial data, reference Euler angles (in DCM), reference quaternions as well as the sampling timestamps are logged via an internal-configured SD card which can be accessed via the onboard USB interface. In the following experiments, the sampling frequencies of the IMU and AHRS are set jointly to 500Hz. Validations and comparisons are carried out on a MacBook Pro Mid-2015 with the configuration of an i7-8core CPU, 16GB RAM and 512G SSD. The MATLAB r2016b software is used

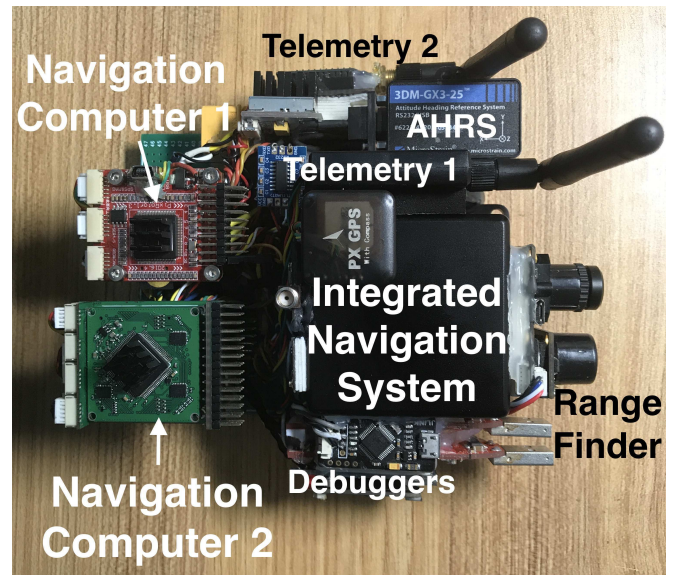


Fig. 4: Designed hardware for validation of proposed algorithm.

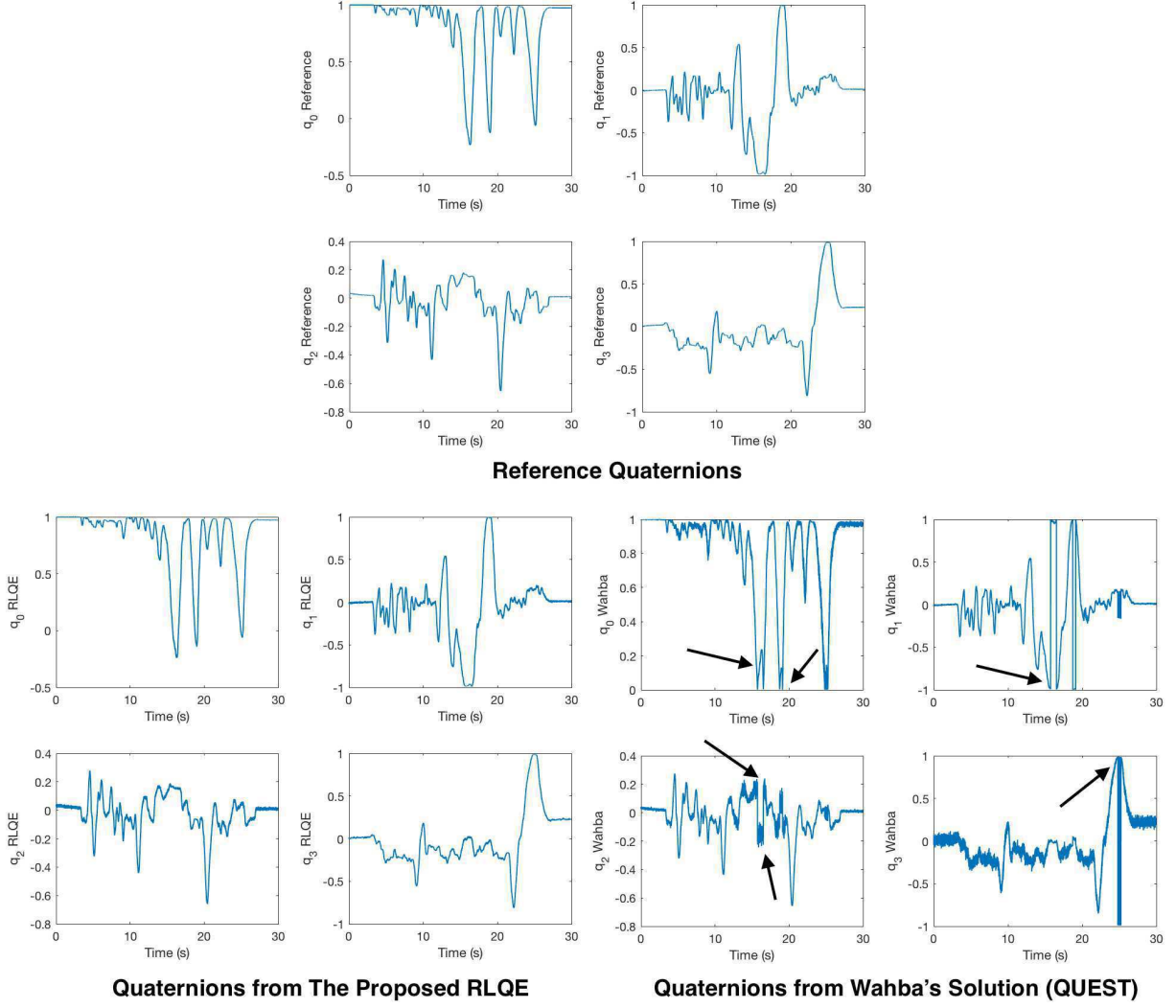


Fig. 3: Estimated quaternions from the proposed RLQE and Wahba's solution as well as the reference quaternions. The estimated quaternion from RLQE is more continuous with less noise density.

4.1.1 Simulational Experiment: In this sub-section, we use the golden reference DCM from the AHRS to generate the simulated data samplings via

$$\begin{aligned} \mathbf{b}_{sim,1} &= \mathbf{C}_{true} \mathbf{r}_1 + \epsilon \\ \mathbf{b}_{sim,2} &= \mathbf{C}_{true} \mathbf{r}_2 + \epsilon \end{aligned} \quad (52)$$

where \mathbf{C}_{true} is the reference DCM and ϵ is the noise. The continuous reference quaternions are also acquired from the device. The standard deviations of all the sensor axes are set to 0.01 while the initial covariance of quaternion is set to \mathbf{I} . In this experiment, the configurations of the reference vectors and weights are the same with that in last section. Initialization of RLQE is carried out before the attitude evolution is propagated. The refinement constant j is set to 3 to ensure the positive definiteness of covariance. The empirical outlier-rejection constant is set to $c = 1$ for normal motion. Reference vectors of vector observations are randomly computed. In this experiment, 4 pairs of vector observations are generated for comparison.

The attitude quaternions from two different algorithms i.e. the proposed RLQE and Wahba's solution (here we use the QUEST) are compared and shown in Fig. 3. The calculated Euler angles are plotted in Fig. 5. Clearly, the estimated quaternions from Wahba's solution are full of data jumpings. The reason has been described before in last section. As we can see, since the quaternions from Wahba's solution are not continuous in time domain, the estimated Euler angles have relatively large errors.

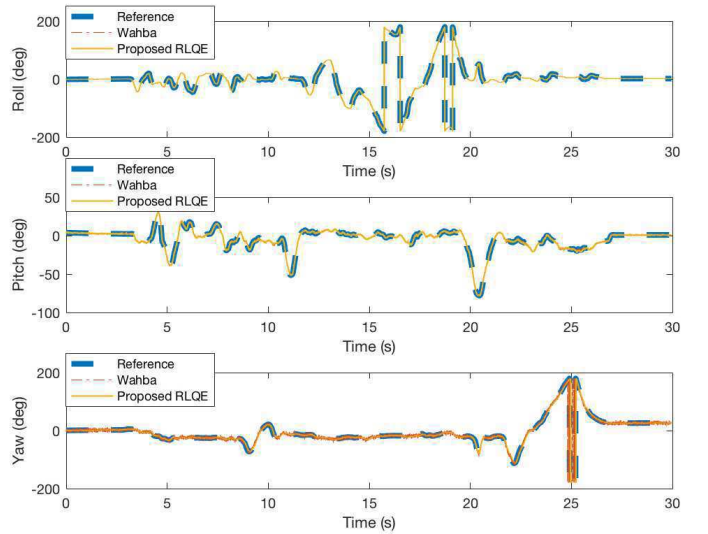


Fig. 5: Estimated Euler angles from the proposed RLQE and Wahba's solution.

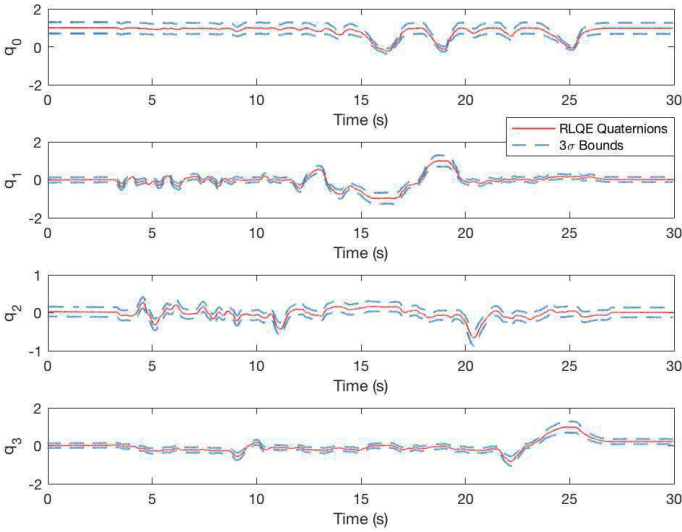


Fig. 6: Estimated quaternions with their 3σ bounds from RLQE.

However, the proposed RLQE does not face such dilemma since it uses the sub-optimal transformation on \mathbb{R}^4 . This proves that the proposed RLQE is more effective than Wahba's solution when the reference vectors almost coincide with each other. The variance information is also obtained generating the Fig. 6.

The original variance of the quaternion is defined by $\Sigma_{q_{init}} = 0.0001\mathbf{I}$ since the quaternion is well-initialized. This figure validates the correctness of the variance analysis of the RLQE proposed in former sections. Due to this, it is believed that in later applications, the RLQE can be fused with other sensors via optimal filtering like Kalman filtering [45]. Also, by using (42), the estimated angular rates are plotted in Fig. 7. We may find out that the estimated angular rates well coincide with the data from gyroscope. Also, it is seen that the variance of the estimated angular rate from RLQE is smaller than that of Wahba's solution (see arrows in figure). This indirectly reflects that the estimated quaternion from RLQE has smaller variance than that from Wahba's solution.

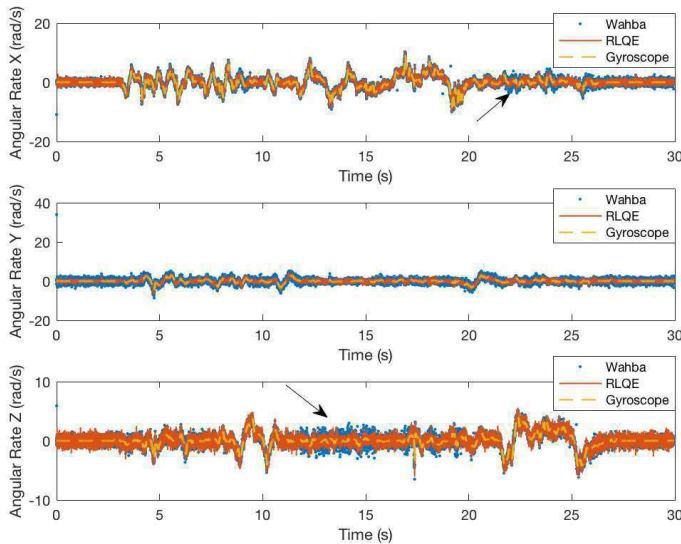


Fig. 7: Estimated angular rates from RLQE and Wahba's solution.

4.1.2 Accelerometer and Magnetometer: Sudden Sensor Failure: The accelerometer and magnetometer are two vital sensors for both satellite attitude determination and consumer electronics [14, 46]. The integration of this two sensors is employed for compensation of in-run biases inside the gyroscope. Based on the

proposed RLQE, it is able to fuse the raw data from the two sensors together and further generate the attitude and angular rate estimation. Using the inertial data acquired in last experiment, the raw data are processed via the 30-order and 5-order low-pass filters (LPFs) respectively. The commitment of adding LPFs to the sensor outputs is a common technique in engineering practice as it decreases the influence of outer disturbances [47]. In order to get the variance of the accelerometer and magnetometer, the device was put still on the experimental table for 10 minutes while the data acquisition system obtained the time series of the raw data. The standard deviations of the two sensors' data are computed as

$$\begin{cases} \sigma_{a_x} = 0.008 \\ \sigma_{a_y} = 0.009 \\ \sigma_{a_z} = 0.008 \end{cases}, \begin{cases} \sigma_{m_x} = 0.014 \\ \sigma_{m_y} = 0.016 \\ \sigma_{m_z} = 0.011 \end{cases} \quad (53)$$

where $\mathbf{A}^b = (a_x, a_y, a_z)^\top$ and $\mathbf{M}^b = (m_x, m_y, m_z)^\top$ are sensor measurements from accelerometer and magnetometer in body frame b respectively.

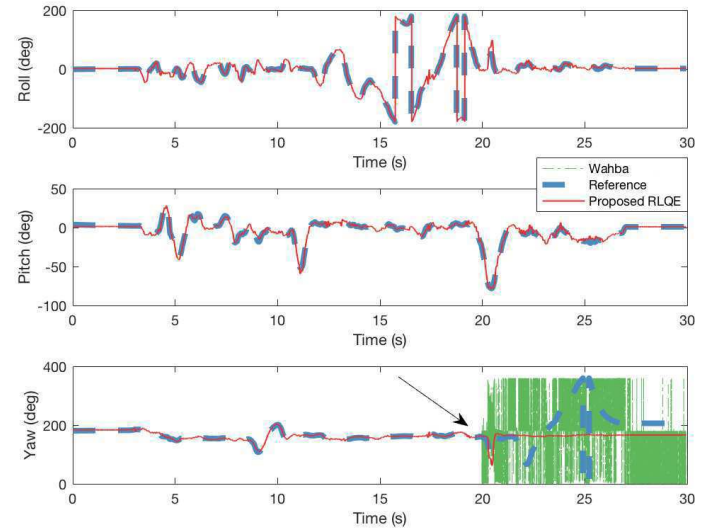


Fig. 8: Estimated Euler angles from accelerometer and magnetometer.

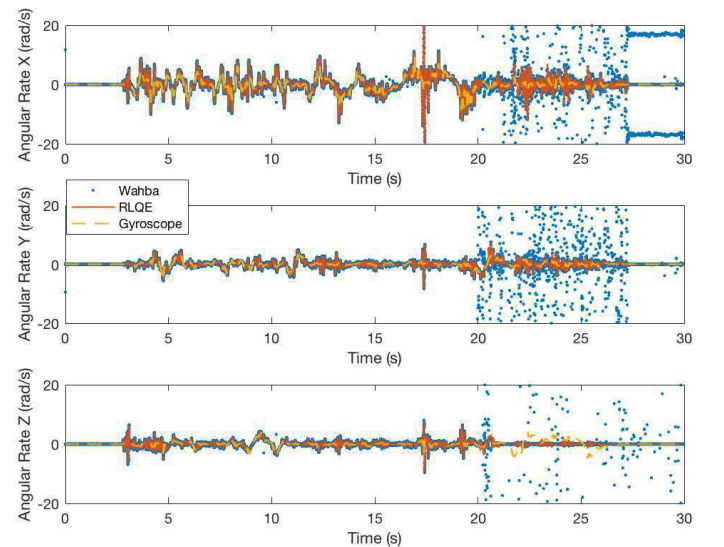


Fig. 9: Estimated angular rates from accelerometer and magnetometer.

The reference vectors of the accelerometer is given by $\mathbf{A}^r = (0, 0, 1)^T$ while that of the magnetometer is computed as $\mathbf{M}^r = (0.60311, 0, -0.79766)^T$ according to the World Magnetic Model 2015 (WMM-2015, [48]). The included angle between \mathbf{A}^r and \mathbf{M}^r is 142.907226° . Here we simulate a condition that at one random moment, the magnetometer fails forever. The estimated angles and angular rates are plotted respectively in Fig. 8 and 9. The starting point of failure is shown by the arrow. We can see that before sensor failure, the experimental results well fit the reference statistics which reflects that using this strapdown sensor combination, the attitude and angular rate can be accurately computed via RLQE or Wahba's solution. However, as sensor failure happens, with only the accelerometer, the Wahba's solutions turn dramatically and suddenly no longer fit the reference angles. The estimated angular rates are influenced accordingly with sensor failure. Estimated quaternions shown in Fig. 10 and 11 indicate that it is the quaternion that determines the Euler angle performance.

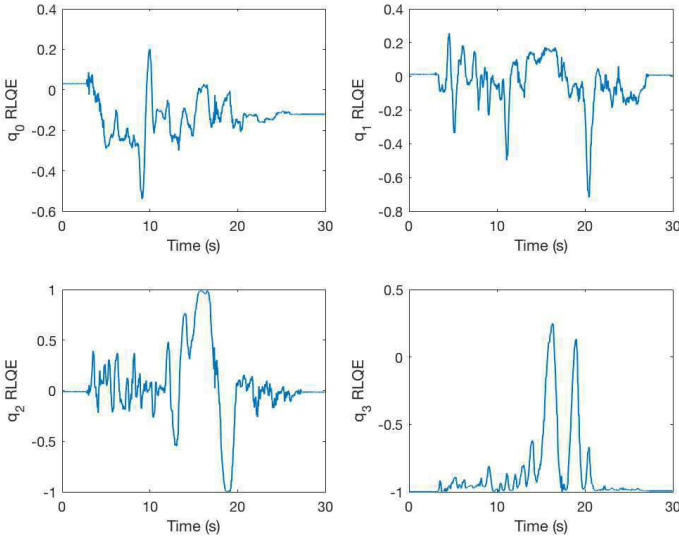


Fig. 10: Estimated quaternions from proposed RLQE.

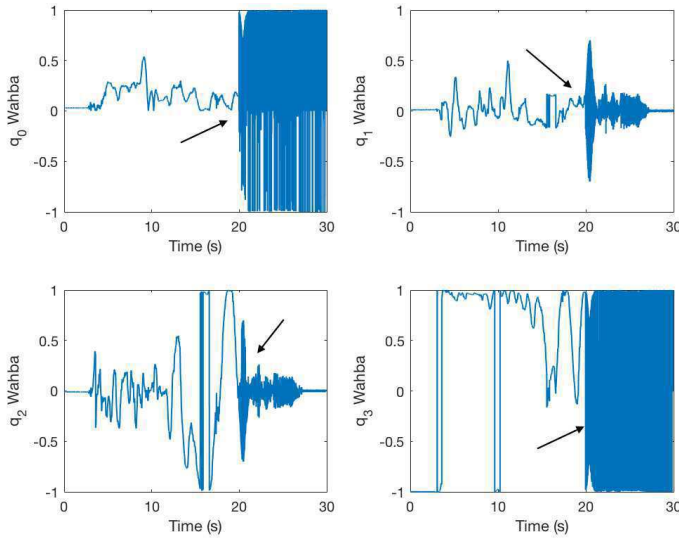


Fig. 11: Estimated quaternions from Wahba's solution.

The estimated quaternions from Wahba's solution start to 'jump' as sensor failure occurs, which shows Wahba's problem can hardly be reliable at this moment. That is to say, some Wahba-based representative algorithms for attitude estimation from such sensor

combination e.g. Yun's QUEST-KF [49] may diverge in this condition. Replacing conventional techniques, RLQE turns out to be a powerful tool dealing with this problem. It maintains continuous, smooth and accurate, compared with reference angles, which verifies its high robustness.

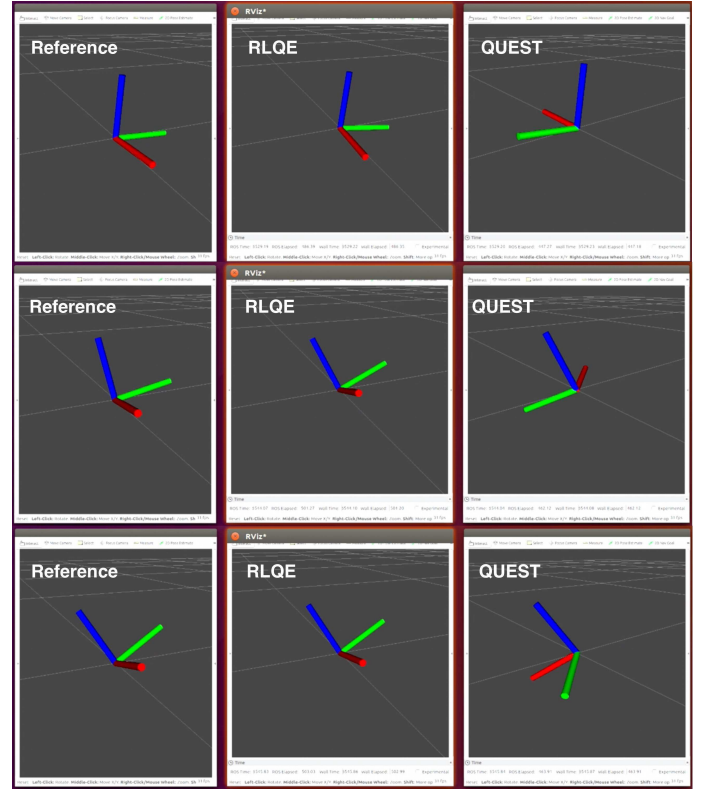


Fig. 12: Estimation results of RLQE and QUEST facing critical sensor configurations.

The dynamical experimental results validated with a mere pair of vector observations are logged in a video. In this video, the algorithms are implemented on a Linux embedded computer where the codes are programmed within the Robotic Operating System (ROS) framework. Some characteristic pictures are listed in Fig. 12, showing the superiority of the proposed RLQE with respect to Wahba's solution. The audience may observe these results on the URL presented in the running head of the first page for detailed information.

4.2 Comparison on RLQE-KF

The combination of RLQE and Kalman filter i.e. RLQE-KF is a competitive filtering technique in face of attitude estimation from rate gyroscope and vector observation pairs, since it is intuitive and simple. Apparently, from last section, we have seen that Wahba's solution can not overcome its internal drawback when critical sensor configuration or failure takes place. In this section, the RLQE-KF is compared to other representative methods using vector observations. Here we choose the Mahony's SO3 complementary filter [50] and Choukroun's quaternion Kalman filter (qKF, [41]). The Mahony's SO3 filter is actually an algorithm on SO3 regardless of the weights. Choukroun's qKF exhibits the stochastic characteristics of the measurement model from each pair of vector observations. In this section, two pairs of vector observations are simulated via reference data in section B, with random reference vectors that have large included angle. The complementary gain of SO3 filter is tuned to 0.1 while the internal parameter of qKF is set to $\alpha = 0.0001$. The

variance of the gyroscope is measured as

$$\begin{cases} \sigma_{gyro,x} = 0.00022 \\ \sigma_{gyro,y} = 0.00025 \\ \sigma_{gyro,z} = 0.00013 \end{cases} \quad (54)$$

The vector observations are generated with the standard deviation of 0.001. The refinement constant j of RLQE is set to 3 ensuring the covariance's positive definiteness. Calculated Euler angles are plotted in Fig. 13. The plotted attitude estimation results indicate that the estimation results more or less fit the reference angles. The root mean-squared errors (RMSE) are summed up in Table 1.

Table 1 Attitude RMSE

Sources	Roll	Pitch	Yaw
SO3 Filter	3.786620°	0.936678°	0.425984°
qKF	2.741016°	1.845730°	7.767874°
RLQE-KF	0.971208°	0.911189°	0.798750°

As we can see, the RLQE-KF has the best relative accuracy compared with other two algorithms. The qKF's accuracy is not so satisfactory while SO3 filter is basically feasible for real applications. This shows that the RLQE-KF can well combine the RLQE and quaternion kinematic model together.

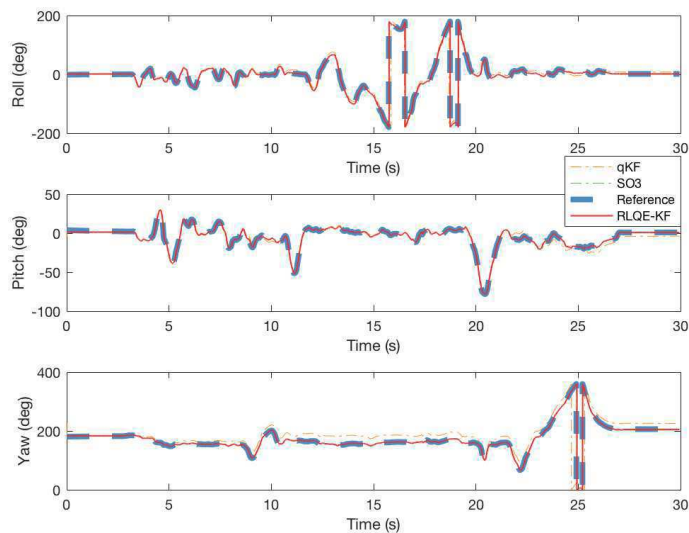


Fig. 13: Estimated results from RLQE-KF and representative algorithms.

4.3 Computation Efficiency Evaluation

Since the proposed RLQE is a linear attitude estimator, the computation speed will be less than that of Wahba's solution when there are few sensor observations. In this sub-section, the two algorithms i.e. QUEST and the proposed RLQE are carried out for 10000 times respectively for each group of vector observations. With increasing amounts of vector observations, there are 10 groups simulated. The following figure describes the mean time consumption of the RLQE and QUEST.

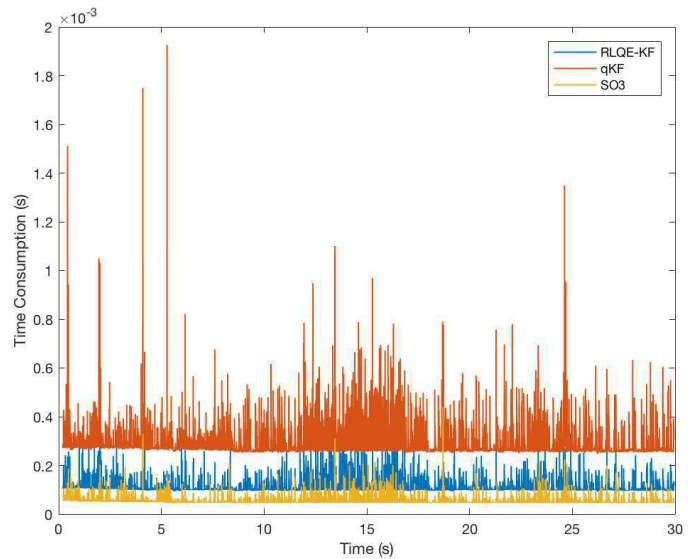


Fig. 14: Time consumption of RLQE-KF, qKF and SO3 filter.

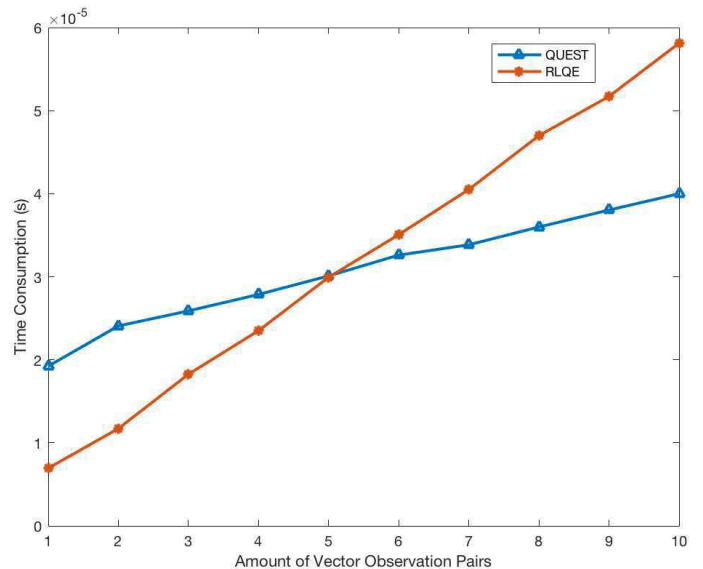


Fig. 15: Time consumption of QUEST and the proposed RLQE.

It is seen from the figures that the two algorithms both have linear computation complexities i.e. $O(n)$. When there are or less than 5 pairs of vector observations, the RLQE seems to be much faster than QUEST. However, as the amount increases, the advantage of the QUEST on time consumption becomes more and more overriding with respect to that of RLQE. This is because in such occasions, the RLQE requires more and more matrix multiplications and thus consumes more and more computation time. It should be noted that the slope of RLQE's time consumption is larger than that of QUEST's. Hence, we can see that when there are few pairs of vector observations the best choice would be the RLQE especially when there is a single vector observation pair. When applying RLQE-KF with gyroscope, the time consumption comparisons are shown in Fig. 14. We can see the SO3 complementary filter has the least time consumption while the qKF consumes the most. However, as SO3 filter can not give any information of covariance, it can hardly be used in highly reliable systems with quality monitoring. The proposed RLQE-KF can provide the users with these data which helps checking the status of the attitude estimator. That is to say RLQE finds a balance between the accuracy and time consumption.

5 Conclusion

This paper revisits the attitude estimation problem from vector observation pairs. Based on our previous findings, the recursive linear quaternion transformation a single vector measurement is presented to overcome shortcomings of classical Wahba's solutions. Mandatory proofs are given to show the continuity of the proposed linear quaternion model. Variance analysis is given to describe the stochastic characters of the obtained quaternion. Analytic quaternion covariance propagation formula from single vector measurement sequences are derived. Supervised covariance propagation is proposed to ensure the positive definiteness. With above studies, the recursive multi-vector attitude estimation theory is established that builds up the framework of the Recursive Linear Quaternion Estimator (RLQE). The presentation of covariance presents a natural motivation of a parallel Kalman filter (RLQE-KF). Starting from numerical examples, the experimental evaluations are given detailedly to show the properties of the RLQE and RLQE-KF regarding their accuracy, continuity, robustness and variance bounds. It is investigated that RLQE maintains the same attitude estimation accuracy with Wahba's solution (QUEST, for representative) but with smaller variance bounds. When applied in critical cases, the Wahba's solutions show a great deal of drawbacks, which can be easily detected and overcome by the proposed RLQE. The RLQE is then tested in a dead-reckoning experiment. The results show that under specific sensor configuration, the robotic navigation ability of RLQE is much better than that of Wahba's solution. Finally, the execution time consumption of the two algorithms is studied showing that when there are few vector observation pairs the RLQE would be more suitable while in opposite the QUEST may be faster. The overall testing results show that the proposed algorithm can be applied in highly reliable robotic tasks and is much more superior to conventional algorithms.

Acknowledgment

This research is supported by National Natural Science Foundation of China under the grant numbers of 41604025 and 61450010 and is also supported by State Key Laboratory of Geodesy and Earth's Dynamics (Institute of Geodesy and Geophysics, Chinese Academy of Sciences) Grant No. SKLGED2018-3-2-E. Prof. Guobin Chang and Prof. Yuhua Cheng gave construction regarding the technical theory and presentation of this paper. We thank them for their help.

6 References

- 1 Fletcher LN. Saturn's seasonal atmosphere. *Astronomy & Geophysics* 2017; 58(4): 4–26.
- 2 Lebreton JP, Witasse O, Sollazzo C et al. An overview of the descent and landing of the Huygens probe on Titan. *Nature* 2005; 438(7069): 758.
- 3 Chang G, Xu T, Wang Q et al. GNSS attitude determination method through vectorisation approach. *IET Radar, Sonar & Navigation* 2017; 11(10): 1477–1482.
- 4 Zhou Z, Li Y, Fu C et al. Least-squares support vector machine-based Kalman filtering for GNSS navigation with dynamic model real-time correction. *IET Radar, Sonar & Navigation* 2017; 11(3): 528–538.
- 5 Hegde GM, Ye C, Robinson Ca et al. Computer-vision-based wheel sinkage estimation for robot navigation on lunar terrain. *IEEE/ASME Transactions on Mechatronics* 2013; 18(4): 1346–1356.
- 6 Reinstein M and Hoffmann M. Dead reckoning in a dynamic quadruped robot based on multimodal proprioceptive sensory information. *IEEE Transactions on Robotics* 2013; 29(2): 563–571.
- 7 Kolomenkin M, Pollak S, Shimshoni I et al. Geometric voting algorithm for star trackers. *IEEE Transactions on Aerospace and Electronic Systems* 2008; 44(2): 441–456.
- 8 Lee JK and Park EJ. A fast quaternion-based orientation optimizer via virtual rotation for human motion tracking. *IEEE Transactions on Biomedical Engineering* 2009; 56(5): 1574–1582.
- 9 Yun X, Calusdian J, Bachmann ER et al. Estimation of human foot motion during normal walking using inertial and magnetic sensor measurements. *IEEE Transactions on Instrumentation and Measurement* 2012; 61(7): 2059–2072.
- 10 Wu J, Zhou Z, Chen J et al. Fast Complementary Filter for Attitude Estimation Using Low-Cost MARG Sensors. *IEEE Sensors Journal* 2016; 16(18): 6997–7007.
- 11 Oshman Y and Carmi A. Attitude Estimation from Vector Observations Using a Genetic-Algorithm-Embedded Quaternion Particle Filter. *Journal of Guidance, Control, and Dynamics* 2006; 29(4): 879–891.
- 12 Shuster MD. Filter QUEST or REQUEST. *Journal of Guidance, Control, and Dynamics* 2009; 32(2): 643–645.
- 13 Zlotnik DE and Forbes JR. Nonlinear Estimator Design on the Special Orthogonal Group using Vector Measurements Directly. *IEEE Transactions on Automatic Control* 2017; 62(1): 149–160.
- 14 Fourati H, Manamanni N, Afifal L et al. Complementary Observer for Body Segments Motion Capturing by Inertial and Magnetic Sensors. *IEEE/ASME Transactions on Mechatronics* 2014; 19(1): 149–157.
- 15 Bras S, Cunha R, Vasconcelos JF et al. A Nonlinear Attitude Observer Based on Range and Inertial Measurements. *IEEE Transactions on Robotics* 2011; 27(4): 664–677.
- 16 Chang L, Hu B, Chang G et al. Multiple Outliers Suppression Derivative-Free Filter Based on Unscented Transformation. *Journal of Guidance, Control, and Dynamics* 2012; 35(6): 1902–1906.
- 17 Sabatini AM. Quaternion-based extended Kalman filter for determining orientation by inertial and magnetic sensing. *IEEE Transactions on Biomedical Engineering* 2006; 53(7): 1346–1356.
- 18 Crassidis J and Markley FL. Unscented Filtering for Spacecraft Attitude Estimation. *Journal of Guidance, Control, and Dynamics* 2003; 26(4): 536–542.
- 19 Markley FL, Crassidis JL and Cheng Y. Nonlinear Attitude Filtering Methods. In *IAAA Guidance, Navigation, and Control Conference and Exhibit 15 - 18 August 2005, San Francisco, California*. August. ISBN 978-1-62410-056-7.
- 20 Crassidis JL, Markley FL and Cheng Y. Survey of Nonlinear Attitude Estimation Methods. *Journal of Guidance, Control, and Dynamics* 2007; 30(1): 12–28.
- 21 Shuster MD and Oh SD. Three-axis attitude determination from vector observations. *Journal of Guidance, Control, and Dynamics* 1981; 4(1): 70–77.
- 22 Markley FL. Attitude determination using vector observations - A fast optimal matrix algorithm. *The Journal of the Astronautical Sciences* 1993; 41(2): 261–280.
- 23 Markley FL. Attitude Determination using Vector Observations and the Singular Value Decomposition. *The Journal of the Astronautical Sciences* 1988; 36(3): 245–258.
- 24 Mortari D. ESOQ: A Closed-Form Solution to the Wahba Problem. *The Journal of the Astronautical Sciences* 1997; 45(2): 195–204.
- 25 Wu J, Zhou Z, Gao B et al. Fast Linear Quaternion Attitude Estimator Using Vector Observations. *IEEE Transactions on Automation Science and Engineering* 2018; 15(1): 307–319.
- 26 Forbes JR and de Ruiter AHJ. Linear-Matrix-Inequality-Based Solution to Wahba's Problem. *Journal of Guidance, Control, and Dynamics* 2015; 38(1): 147–151.
- 27 Yang Y and Zhou Z. An analytic solution to Wahba's problem. *Aerospace Science and Technology* 2013; 30(1): 46–49.
- 28 Wu J, Zhou Z, Li R et al. Attitude Determination Using a Single Sensor Observation : Analytic Quaternion Solutions and Property Discussion. *IET Science, Measurement & Technology* 2017; 11(3): 731–739.
- 29 Cheng Y, Crassidis JL and Landis Markley F. Attitude estimation for large field-of-view sensors. *Advances in the Astronautical Sciences* 2006; 122: 193–208.
- 30 Cheng Y and Shuster MD. Improvement to the Implementation of the QUEST Algorithm. *Journal of Guidance, Control, and Dynamics* 2014; 37(1): 301–305.
- 31 Chang G, Xu T and Wang Q. Error analysis of Davenport's q method. *Automatica* 2017; 75: 217–220.
- 32 Markley FL and Mortari D. How to estimate attitude from vector observations. *Advances in the Astronautical Sciences* 2000; 103(PART III): 1979–1996.
- 33 Zhou Z, Wu J, Wang J et al. Optimal, recursive and sub-optimal linear solutions to attitude determination from vector observations for gnss/accelerometer/magnetometer orientation measurement. *Remote Sensing* 2018; 10(3): 377.
- 34 Ma SD. A self-calibration technique for active vision systems. *IEEE Transactions on Robotics and Automation* 1996; 12(1): 114–120.
- 35 Mirzaei FM and Roumeliotis SI. A Kalman-filter-based algorithm for IMU-camera calibration: observability analysis and performance evaluation. *IEEE Transactions on Robotics* 2008; 24(5): 1143–1156.
- 36 Chang G. Total least-squares formulation of Wahba's problem. *Electronics Letters* 2015; 51(17): 1334–1335.
- 37 Oppenheim AV. *Discrete-time signal processing*. Pearson Education India, 1999.
- 38 Huang Y, Zhang Y, Li N et al. Robust student's t based nonlinear filter and smoother. *IEEE Transactions on Aerospace and Electronic Systems* 2016; 52(5): 2586–2596.
- 39 Huang Y, Zhang Y and Wang X. Kalman-Filtering-Based In-Motion Coarse Alignment for Odometer-Aided SINS. *IEEE Transactions on Instrumentation and Measurement* 2017; : 1–14.
- 40 Martinelli A. Vision and IMU Data Fusion : Closed-Form Solutions for Attitude, Speed, Absolute Scale, and Bias Determination. *IEEE Transactions on Robotics* 2012; 28(1): 44–60.
- 41 Choukroun D, Bar-Itzhack IY and Oshman Y. Novel quaternion Kalman filter. *IEEE Transactions on Aerospace and Electronic Systems* 2006; 42(1): 174–190.
- 42 Maybeck PS. *Stochastic models, estimation, and control*, volume 1. Academic Press, 1979. ISBN 0124807011.
- 43 Chang L, Qin F and Li A. A Novel Backtracking Scheme for Attitude Determination-Based Initial Alignment. *IEEE Transactions on Automation Science and Engineering* 2014; 12(1): 384–390.
- 44 Vasconcelos JF, Carreira B, Silvestre C et al. Discrete-time complementary filters for attitude and position estimation: Design, analysis and experimental validation. *IEEE Transactions on Control Systems Technology* 2011; 19(1): 181–198.
- 45 Zhou Z, Li Y, Liu J et al. Equality constrained robust measurement fusion for adaptive kalman-filter-based heterogeneous multi-sensor navigation. *IEEE Transactions on Aerospace and Electronic Systems* 2013; 49(4): 2146–2157.
- 46 Makni A, Fourati H and Kibangou A. Energy-aware Adaptive Attitude Estimation Under External Acceleration for Pedestrian Navigation. *IEEE/ASME Transactions on Mechatronics* 2015; 4435(c): 1–1.

- 47 Zhou Z, Li Y, Zhang J et al. Integrated Navigation System for a Low-Cost Quadrotor Aerial Vehicle in the Presence of Rotor Influences. *Journal of Surveying Engineering* 2017; 143(1): 05016006.
- 48 Maus S, Macmillan S, McLean S et al. The us/uk world magnetic model for 2010-2015 2010; .
- 49 Yun X and Bachmann E. Design, Implementation, and Experimental Results of a Quaternion-Based Kalman Filter for Human Body Motion Tracking. *IEEE Transactions on Robotics* 2006; 22(6): 1216–1227.
- 50 Mahony R, Hamel T and Pflimlin JM. Nonlinear complementary filters on the special orthogonal group. *IEEE Transactions on Automatic Control* 2008; 53(5): 1203–1218.